



# Parametric investigation of electropolishing to enhance the surface characteristics of maraging steel with organic electrolytes

Abhinav Kumar<sup>1</sup> · Suraj Kumar<sup>1</sup> · Manas Das<sup>1</sup>

Received: 22 September 2021 / Accepted: 5 July 2022 / Published online: 14 July 2022  
© The Author(s), under exclusive licence to Springer-Verlag London Ltd., part of Springer Nature 2022

## Abstract

Maraging steel 300 is widely used in aircraft, tools, and automotive industries, which requires a polished surface for better performance. In conventional methods of polishing, the abrasives directly contact the workpiece surface and deteriorate its property. Thus, a nonconventional method like electropolishing (EP), is utilized to finish maraging steel with acetic acid and perchloric acid mixed in the volume of 3:1. Linear sweep voltammetry (LSV) is performed to determine the passive region that gives the best electropolishing performance. Different parameters, namely temperature, agitation, and polishing time and their effect on surface roughness and surface reflectance, are observed during EP. The optimized process parameters, which give the best EP performance, are the temperature at 60 °C, rotation of magnetic stirrer at 400 rpm, and polishing time of 6 min. An improvement of 56.25% in surface roughness and 60.3% in surface reflectance from its initial value of 21% is observed. EP makes the surface hydrophilic as the contact angle changes from 111.2 to 68.6°. X-ray photoelectron spectroscopy analysis suggests that after EP, thick passive layer forms on the surface, which helps in increasing corrosion resistance.

**Keywords** Maraging steel · Electropolishing · Surface roughness · Surface reflectance · Contact angle

## 1 Introduction

EP is a nonconventional polishing method that follows anodic dissolution. The polishing setup comprises an anode (sample to be electropolished), a cathode (tool), and an electrolyte. In EP, the electrolyte mainly consists of viscous acidic fluid. During EP, the hydrogen gas is evolved at the tool and oxygen gas at the workpiece, followed by anodic dissolution, as shown in Fig. 1. Due to the diffusive mechanism in EP, as explained by Jacquet's viscous film theory [1], a viscous film forms over the workpiece surface. This viscous layer increases electrical resistance for anodic dissolution. A thick layer forms on the valley, whereas a thin layer forms on the anode's protruding surface. Due to this difference in the layer thickness, a higher resistance for anodic dissolution for valleys than protruding surfaces is observed. This creates a polishing effect by removing the protruding surface first, followed by the valley. Hence, the surface is leveled and polished during EP [2]. It does not

change the actual property of the bulk metal and also forms a stable passive oxide layer, which increases the corrosion resistance [3].

During electropolishing, oxygen gas evolves at the anode forming bubbles and moves away the electropolishing solution from the anode film surface. Hence, the protruding surface on the workpiece dissolves faster, while the valley remains inaccessible [4]. EP does not change the crystallographic and grain-boundary structure of the bulk material and never induces any residual stress, which makes it different from other polishing methods [5]. This advantage of EP is utilized as a post-processing method for components fabricated by thermal-induced processes like laser beam machining (LBM), Electric discharge machining (EDM), etc. This paper performs EP of maraging steels as it offers competitive alternative materials for aerospace structures while exhibiting ultra-high-strength and good corrosion resistance [6]. In additive manufacturing, it is widely used as raw powders to fabricate complex parts [7].

Oliveira et al. [8] used the powder bed fusion process for 3D printing of maraging steel 300. The effects of cutting parameters like feed per tooth and cutting speeds on the surface conditions, namely average roughness and residual stress during milling, were investigated. Surface roughness

✉ Manas Das  
manasdas@iitg.ac.in

<sup>1</sup> Department of Mechanical Engineering, Indian Institute of Technology Guwahati, Guwahati, India

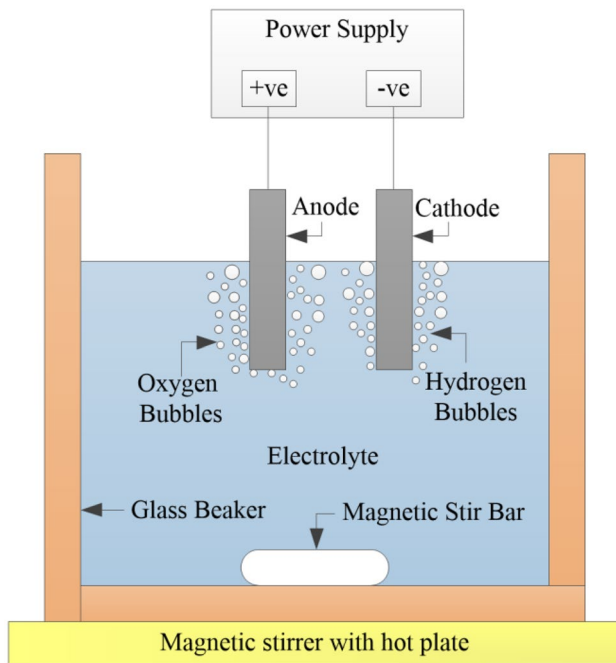


**Fig. 1** Schematic of the electropolishing setup

of  $3.30\ \mu\text{m}$  was obtained after additive manufacturing. Milling was used as a post-processing technique to reduce the surface roughness to  $0.31\ \mu\text{m}$  at  $250\ \text{m/min}$  cutting speeds and  $0.02\ \text{mm/tooth}$  feed per tooth. Compared to EP, the conventional milling process directly contacts the workpiece, changes the workpiece's grain structure completely, and induces compressive residual stress.

Li et al. [9] polished maraging steel by micro-grinding and achieved a minimum roughness of  $0.67\ \mu\text{m}$ . They found that the metal surface property changes drastically while polishing at a very high speed. They proposed a small grinding wheel with a very low rotating speed to avoid this. Also, residual stress was induced on the workpiece surface while polishing by micro-grinding [9]. These disadvantages of conventional polishing methods make way for researchers to proceed with nonconventional polishing methods.

Very little literature is available that discusses the electropolishing of maraging steel. As it is a Ni-based alloy, the author tries to find the electrolyte for the electropolishing of Ni-based alloys. Huang et al. [10] utilized perchloric-acetic mixed acids electrolytes to investigate the EP behavior of Inconel 718 alloy. Anodic polarization curves at different concentrations of perchloric acid ( $\text{HClO}_4$ ) were analyzed, and it was concluded that more than 50 vol.% of  $\text{HClO}_4$  provides better anodic dissolution. Electropolishing enhances the

corrosion resistance of Inconel 718 alloy. For Ni-based alloys, perchloric-acetic acid mixtures are generally used as an electrolyte [10–12]. Aksu et al. [12] had electropolished Fe–Ni–Co alloy in perchloric acid solution with acetic acid as a solvent. Linear sweep voltammetry was performed to find the current density for different concentrations of perchloric acid. An investigation was conducted to analyze the effect of electrolyte concentration, current density, and bath temperature on surface roughness and thickness change. Surface roughness of  $0.05\ \mu\text{m}$  is achieved.

Wang et al. [13] had investigated the parameters of electropolishing on the surface quality of a Ni–Ti shape memory alloy after milling. It was observed that the better the initial surface homogeneity, the better would be EP effect. Methanol-perchloric acid mixture was used as an electrolyte to achieve a minimum roughness of  $0.279\ \mu\text{m}$ . Han and Fang [14] had compared NaCl-based electrolyte with  $\text{H}_2\text{SO}_4$ -based electrolyte for EP of stainless steel 316L. It was observed that the NaCl-based electrolyte has a higher current density, which leads to a higher material removal rate. Surface roughness of  $20.4\ \text{nm}$  and  $100\ \text{nm}$  had been achieved for the respective electrolytes.

In the present study, electropolishing of maraging steel is performed. An organic electrolyte solution containing acetic acid with perchloric acid is used for electropolishing. The various parameters like polishing time, temperature, and agitation are analyzed. Linear sweep voltammetry (LSV) is performed to generate the polarization curve for maraging steel at a particular solution. Energy-dispersive X-ray spectroscopy (EDS) analysis is performed to investigate the workpiece surface composition before and after EP. The influence of EP parameters on surface roughness and surface reflectance is also presented. The contact angle of the surface is measured with the help of a goniometer to analyze the workpiece surface's wettability before and after EP. Corrosion behavior of the sample before and after EP is also studied.

## 2 Electropolishing experimental procedure

### 2.1 Experimental setup

The schematic of the proposed electropolishing setup for maraging steel electropolishing is shown in Fig. 1. It is an extended version of the electrochemical machining (ECM) setup. It also contains an electrolyte circulation system and an arrangement for cathode and anode electrodes holding system. A glass container of 100 ml is used

as a chamber for electropolishing. A graphite sheet connected to the power supply’s negative terminal is used as a cathode. The cathode is dipped inside the glass electrolyte chamber. A rectangular maraging steel 300 sheet of dimension 25 mm × 10 mm × 3 mm is used as the anode, which connects to the power supply’s positive terminal. The complete setup is kept over a hot plate with the magnetic stirrer. The hot plate is used to provide the required amount of heat to increase the electrolyte’s temperature. The magnetic bar rotates within the glass chamber with the help of a magnetic stirrer. It agitates the solution during electropolishing. Hence, the dissolved particles are easily cleaned off from the workpiece surface [14]. A DC power supply of 60 V and 20 A rating provides a potential difference between anode and cathode. The actual electropolishing experimental setup is shown in Fig. 2. Table 1 shows the EP process parameters selected for polishing maraging steel. The major influencing parameters are electrolyte temperature, rotation of magnetic stirrer, and polishing time.

As shown in Fig. 3, the flow chart describes the step-by-step process of electropolishing. The first step is the preparation of the sample. The maraging steel is cut by wire-EDM and then mechanically polished consecutively with sandpapers of grit nos: 120, 400, and 600 for eliminating scratch marks and deformed layers from the test samples. The surface is manually cleaned using acetone. Further cleaning is

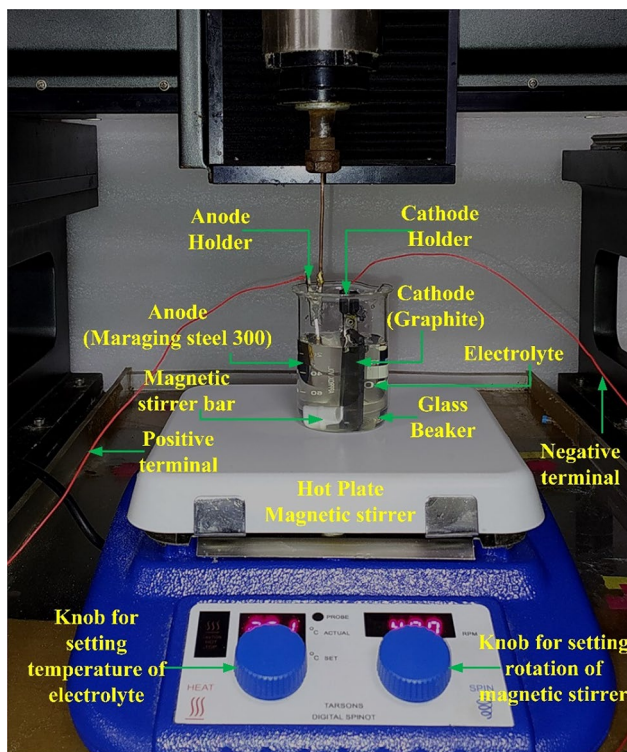


Fig. 2 Experimental setup for EP

Table 1 Electropolishing process parameters

Parameters	Value
Voltage	6 V
Electrolyte	Vol. ratio of acetic acid and Perchloric acid is 3:1
Polishing time	4–10 min
Agitation	0–600 rpm
Temperature	30–75 °C

conducted with deionized water in an ultrasonic cleaner for 15 min. The specimen’s initial surface roughness (Ra) is about 0.272 μm.

### 2.2 Electrochemical analysis

A polarization curve is drawn utilizing linear sweep voltammetry (LSV) to correlate voltage and current during electropolishing. The organic electrolyte, which consists of acetic acid and perchloric acid, is mixed in a volume ratio of 3:1. LSV provides three different zones such as active, passive, and transpassive. An electrochemical workstation (Gamry Instruments) with a three-electrode system, namely working electrode (maraging steel sample), counter electrode (platinum electrode), and reference electrode (Ag/AgCl electrode), is used for LSV. The voltage is swept between 10 and 0 V with a scan rate of 10 mV/s [15]. The potential must be swept in the cathodic direction to avoid any pitting of the electrode surface while achieving reproducible measurements [16].

### 2.3 Analysis of polished surface

The polished surface microstructure and its morphology were analyzed with the help of an optical microscope and field emission scanning electron microscopy

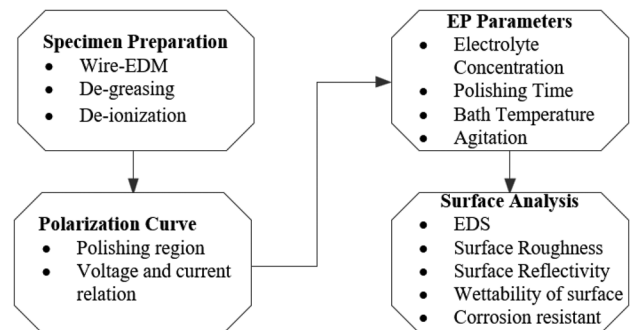


Fig. 3 Flowchart of the electropolishing process

(FESEM). The sample is fixed in the epoxy resin using a cold setting to obtain the grain structure. The specimens were first mechanically polished with sandpapers of grit nos. 120, 400, and 600 to eliminate the test samples' scratch marks and deformed layer. Finally, it is polished in buff cloth with 1  $\mu\text{m}$  diamond paste. For visualizing the microstructure, the sample should be etched. A modified fry reagent consisting of 75 ml of deionized water (DI), 25 ml of hydrochloric acid (36 wt.%), 12.5 ml of nitric acid (68 wt.%), and 0.5 g of copper (II) chloride ( $\text{CuCl}_2$ ) is prepared as the etchant. For the etching of the cold mounted sample, the surface is scrubbed for approximately 60 s with cotton, which is dipped in the solution, and then the surface is cleaned with deionized water and ethanol, followed by hot, dry air [17]. The metallographic structure is inspected with the help of a metallographic optical microscope.

The surface roughness ( $R_a$ ) was measured with the help of a noncontact optical profilometer. The elemental composition is characterized by the help of EDS. Further, the contact angle is measured for the wettability study, i.e., hydrophilicity and hydrophobicity of the polished surface. It is inspected using a goniometer utilizing the sessile method of contact angle measurement. For this purpose, a water drop of 2  $\mu\text{l}$  is placed over the workpiece surface before and after EP [18]. The contact angle can be utilized to calculate the surface energy of the metallic workpiece surface [19]. An angle greater than  $90^\circ$  signifies a hydrophobic surface, and a lesser than  $90^\circ$  signifies hydrophilic.

X-ray photoelectron spectroscopy (XPS) analysis is carried out to study the surface elemental composition before and after EP. The measured XPS spectra were calibrated with respect to C 1 s (284.8 eV) adventitious peak, and the samples were scanned from 0 to 1200 eV with a step size of 1 eV. Higher-resolution spectra are conducted for iron, nickel, and oxygen elements. The Gaussian function is used for background correction.

Corrosion analysis is performed by utilizing the Tafel polarization curve by conducting experiments in potentiostat. The potential is varied from  $-250$  to  $+250$  mV vs. Ag/AgCl with respect to the corrosion potential at a

scan rate of  $10 \text{ mVs}^{-1}$  using 3.5 wt.% of NaCl solution [20]. Various parameters like corrosion potential ( $E_{\text{corr}}$ ) and corrosion current density ( $I_{\text{corr}}$ ) are evaluated from the experimental curve. Table 2 shows the operating conditions during various operations performed to analyze the electropolished surface.

### 3 Results and discussions

EP is performed on the maraging steel 300 sheet. The organic electrolyte consisting of acetic acid and perchloric acid is mixed in a volume ratio of 3:1. The setup for EP is indigenously designed and fabricated. It consists of electrolytes with electrodes. The effect of different parameters such as polishing time, temperature, agitation on surface roughness, and surface reflectance are investigated. The results are discussed in the following subsections.

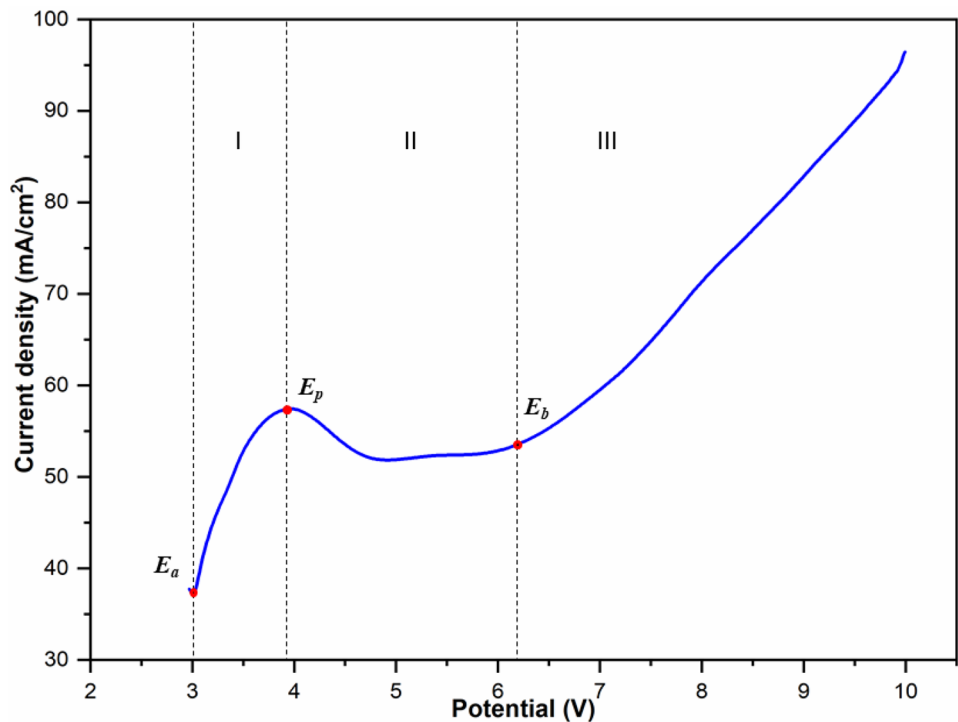
#### 3.1 Anodic polarization behavior of maraging steel

Linear sweep voltammetry (LSV) is performed to determine the anodic polarization behavior of maraging steel, as shown in Fig. 4. Three electrodes system is used to select the region of EP. The polarization curve is conducted by varying the potential from 10 to 0 V with a scan rate of 10 mV/s [21]. The polarization curve obtained in acetic acid and perchloric acid solution in maraging steel consists of three regions (Fig. 4). The region between 3 and 4 V is the active region (I) in which current increases with increased potential. The corresponding potential of 3 V is termed activation potential ( $E_a$ ). The region between 4 and 6.2 V is the passive region (II), where the current is stable for an increase in voltage. The corresponding potential of 4 V is termed passivation potential ( $E_p$ ). After this region, the current increases rapidly in the transpassive region (III). The corresponding potential of 6.2 V is termed breakdown potential ( $E_b$ ). Three sets of experiments are performed to measure the breakdown voltage. An almost similar anodic polarization behavior of maraging steel in acetic acid and perchloric acid is observed for

**Table 2** Operating conditions

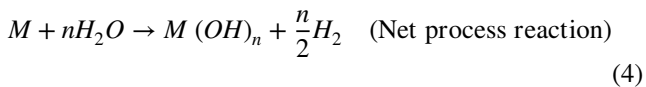
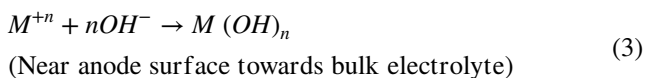
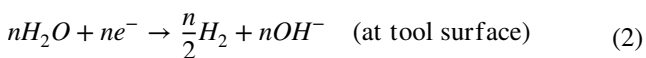
Experiments	Value
Linear sweep voltammetry	Potential range: 10 to 0 V; scan rate: 10 mV/s
Surface reflectance	UV light with a wavelength between 200 and 1000 nm
Contact angle	Waterdrop of 2 $\mu\text{l}$
Tafel polarization	Potential range: $-250$ to $+250$ mV; scan rate: 10 mV/s
Electrolyte for corrosion analysis	3.5 wt.% NaCl solution

**Fig. 4** Anodic polarization behavior of maraging steel in acetic acid and perchloric acid with breakdown voltage at  $6.2 \pm 0.3$  V (after three repetitions)



all three experimentations, with the breakdown voltage measured at  $6.2 \pm 0.3$  V.

As per literature, EP occurs only in the passive region. A viscous film having higher resistance than the electrolyte is formed in the passive region [15]. Region (III) is also termed a gas evolution region where oxygen gas bubbles evolved. The reactions that take place during EP are discussed below in Eq. (1) to (4) [22].



During EP, the metal (M: Fe, Ni) is dissolved by releasing electrons ( $n$ , valency of metal M) (Eq. (1) [23], and these electrons are gained on the cathode surface to produce hydrogen gas ( $H_2$ ) and hydroxyl ions ( $OH^-$ ) (Eq. (2) [24]. These hydroxyl ions combine with metal ions near the anode surface and form metal hydroxides (Eq. (3)). The overall reaction to the EP process is expressed as

Eq. (4). The chemical reactions (i.e., Eqs. ((1)–(4)) are the proposed generalized reactions that occur during electropolishing. These equations show the proposed formation of metal hydroxides. Metal oxides may also be generated at the anode surface, the equations of which are not shown in the present manuscript. Hence, XPS analysis has been performed to find out the generated final products (i.e., metal hydroxides and oxides) and are discussed later in Sect. 3.7.

### 3.2 Effect of electropolishing on the elemental composition of surface

Energy-dispersive X-ray spectroscopy analysis is performed to investigate the elemental composition of maraging steel 300 surfaces before and after EP. The initial surface is cleaned with acetone, followed by an ultrasonic cleaner. EDS analysis of maraging steel before and after EP is shown in Fig. 5a, b. EP is performed at  $60^\circ\text{C}$  with magnetic stirrer bar rotation at 400 rpm.

Table 3 shows the changes in the surface’s elemental compositions before and after EP, which are negligible [25]. However, the subsurface composition is not measured with EDS. An increase in % oxygen composition indicates that an oxide layer is formed on the surface after EP, increasing corrosion resistance [26]. EDS analysis



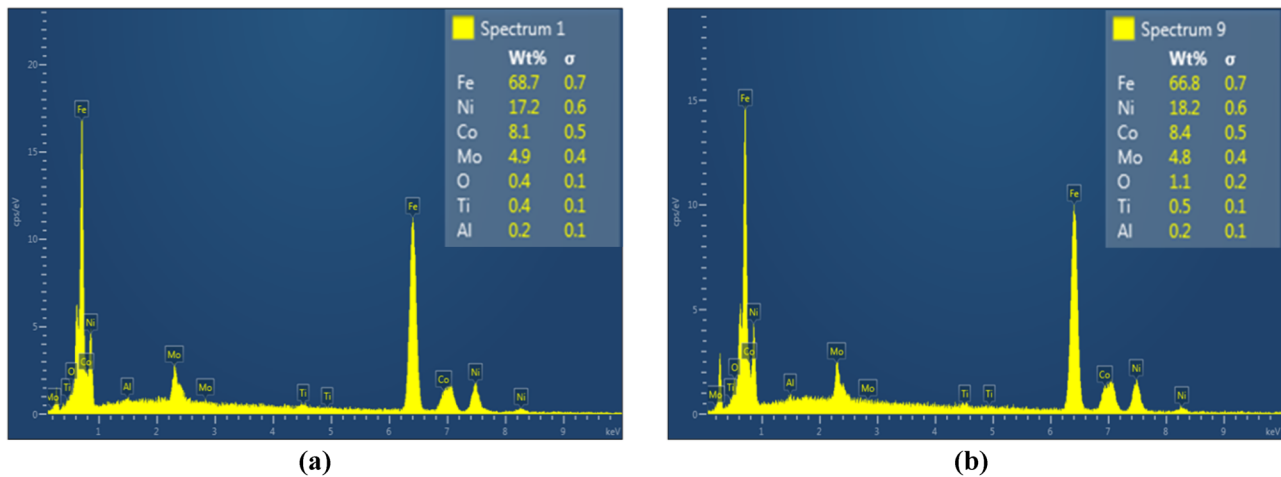


**Fig. 5** EDS analysis of maraging steel at 60 °C with 400 rpm stirrer rotation **a** before and **b** after EP

suggests that after EP, the concentration of  $\text{Ni}^+$  increases, and  $\text{Fe}^+$  decreases at the passive layer [27]. The surface microstructural images of maraging steel before and after EP are shown in Fig. 6a, b, respectively. The microstructure consists of martensite and austenite phases [28]. However, distinct grain boundaries with no scratch marks are visible after EP [4].

### 3.3 Effect of temperature on surface roughness and reflectance

During electropolishing, the temperature has a significant effect on the surface roughness. As the temperature increases, the conductivity of electrolytes increases, which increases the anodic dissolution [29]. The percentage improvement in the surface roughness with temperature has been shown in Fig. 7. As temperature increases, the surface roughness decreases. A

**Table 3** Elemental compositions of maraging steel in wt.% before and after EP

Process element	Before EP		After EP	
	% wt	S.D ( $\sigma$ )	% wt	S.D ( $\sigma$ )
Fe	68.7	0.7	66.8	0.7
Ni	17.2	0.6	18.2	0.6
Co	8.1	0.5	8.4	0.5
Mo	4.9	0.4	4.8	0.4
O	0.4	0.1	1.1	0.2
Ti	0.4	0.1	0.5	0.1
Al	0.2	0.1	0.2	0.1

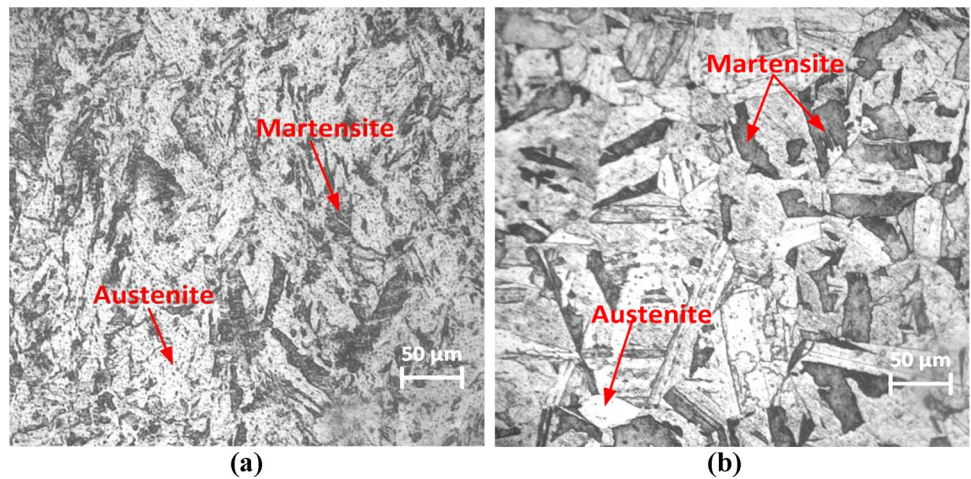
maximum gain of  $55.47 \pm 3\%$  is observed at 60 °C (out of 5 repeated experimentations at the same condition). At higher temperatures, faster anodic dissolution occurs, which leads to pitting the surface. Hence, the surface finish deteriorates. It can be inferred from Fig. 7 that beyond 60 °C, the percentage improvement in surface roughness decreases.

The temperature has a significant effect on surface reflectance during EP. The surface reflectance at various temperatures is shown in Fig. 8. The relative surface reflectance is measured with reference to a highly polished silver surface having 100% reflectivity. The magenta dot line shows the surface reflectance of the unpolished base material. The ultraviolet (UV) light is varied between 1000 and 200 nm. It can be inferred from Fig. 8 that better surface reflectance is observed at 60 °C, having a maximum surface reflectance value of  $58.6 \pm 2\%$  (out of 5 repeated experimentations at the same condition). At a higher temperature, above 60 °C, pitting occurs, decreasing surface reflectance.

### 3.4 Effect of agitation on surface roughness and surface reflectance

The effect of agitation on surface roughness is shown in Fig. 9. A magnetic stirrer is used to provide agitation to the solution during EP. The magnetic bar is rotated from 0 to 600 rpm to see its effect on workpiece surface roughness. Electropolishing was performed at 60 °C for 6 min with a varied magnetic stirrer rotation between 0 and 600 rpm. It can be inferred from Fig. 9 that as the rotational speed increases from 0 to 400 rpm, surface roughness decreases

**Fig. 6** The surface microstructural images of maraging steel 300 using an optical microscope **a** before and **b** after EP



during EP due to the stirring of the electrolyte and further easy removal of the gas bubbles. The maximum improvement in surface roughness is observed as  $56.25 \pm 2\%$  at 400 rpm magnetic bar rotation (out of 5 repeated experimentations at the same condition). With increased rotational speed from 400 to 600 rpm, the viscous layer formed on the anode surface becomes unstable, increasing surface roughness [30].

A comparison of surface reflectance between unpolished and electropolished samples at different rotations (between 0 and 600 rpm) of the magnetic stirrer is shown in Fig. 10. Electropolishing is performed at 60 °C for 6 min. The magenta dot line shows the surface reflectance of the

unpolished base material. The higher the surface finish, the higher will be the surface reflectance. It can be inferred from Fig. 10 that at 400 rpm, maximum reflectance of  $60.3 \pm 3\%$  is observed (out of 5 repeated experimentations at the same condition).

### 3.5 Effect of polishing time on surface roughness and reflectance

The percentage improvement of the surface roughness with polishing time is shown in Fig. 11. The polishing time is varied between 4 and 10 min at an interval of 2 min. It can be inferred from Fig. 11 that as polishing

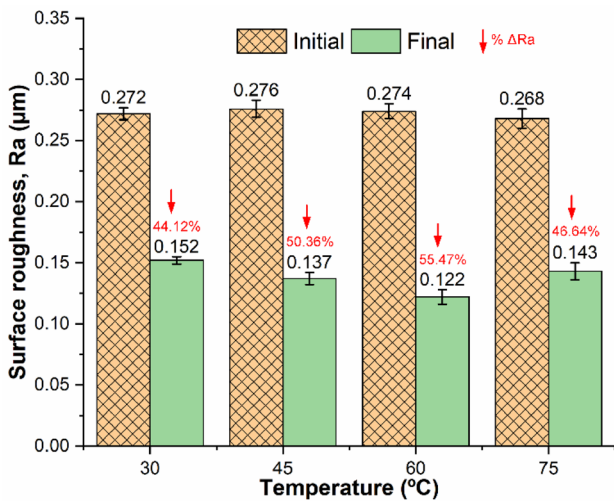


**Fig. 7** Effect of temperature on surface roughness with maximum roughness improvement of  $55.47 \pm 3\%$  at 60 °C (out of 5 repeated experimentations at the same condition)

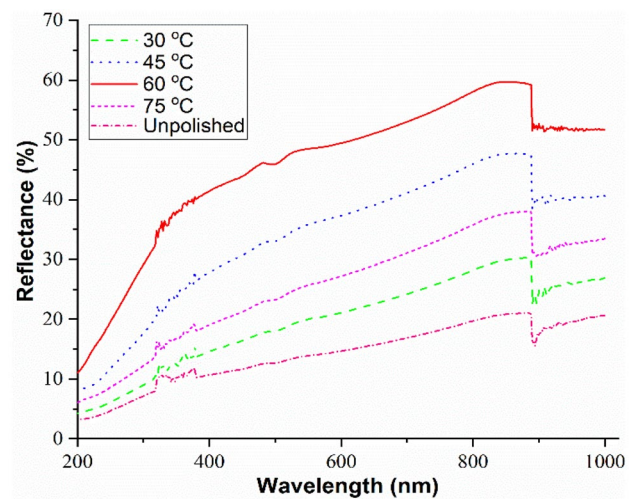


**Fig. 8** Effect of temperature on surface reflectance with a maximum reflectance of  $58.6 \pm 2\%$  at 60 °C (out of 5 repeated experimentations at the same condition)

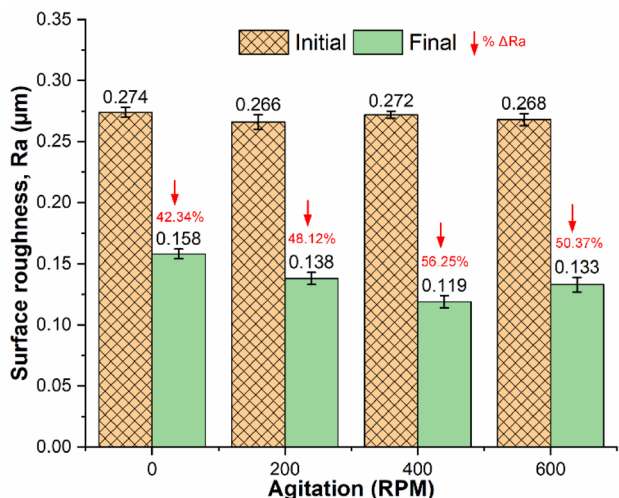


**Fig. 9** Effect of magnetic stirrer agitation (i.e., rotation) on surface roughness with a maximum improvement of  $56.25 \pm 2\%$  at 400 rpm (out of 5 repeated experimentations at the same condition)

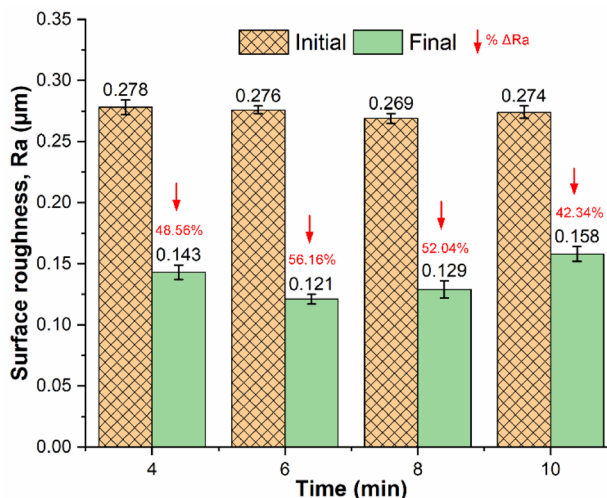


**Fig. 11** Effect of polishing time on surface roughness with a maximum roughness improvement of  $56.16 \pm 2\%$  at 6 min (out of 5 repeated experimentations at the same condition)

time increases, surface finish increases. However, with the rise in polishing time, the amount of material removal also increases. The maximum improvement in surface roughness is obtained as  $56.16 \pm 2\%$  at 6 min of EP (out of 5 repeated experimentations at the same condition). For a longer duration of EP, the amount of anodic dissolution increases, and alloying elements starts leaving the surface, creating pits and deteriorating surface finish [31].

A comparison between the surface reflectance of the electropolished samples at different polishing durations

with the unpolished ones is represented in Fig. 12. Electropolishing is performed at  $60^\circ\text{C}$  at a magnetic stirrer rotation of 400 rpm while varying the polishing time between 4 and 10 min. The maximum reflectance of  $59.7 \pm 3\%$  (out of 5 repeated experimentations at the same condition) is observed for 6 min of electropolishing, as inferred from Fig. 12. The reflectance property of the surface is of great importance for the industries, which requires radiant surface. Higher the reflectance, the higher the ability to reflect the visible, infrared, and ultraviolet light.

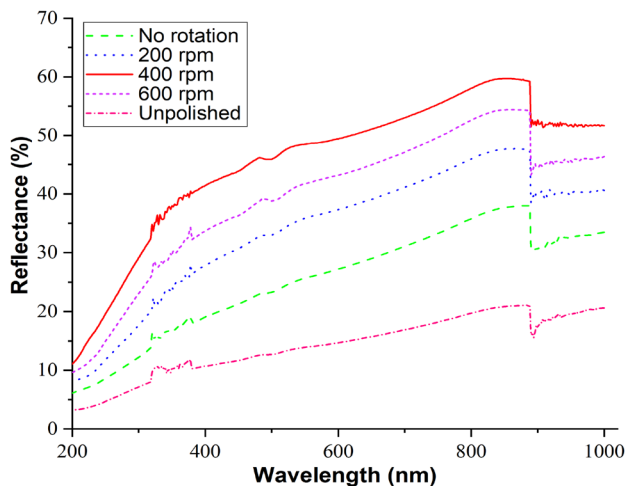


**Fig. 10** Effect of magnetic stirrer agitation (i.e., rotation) on surface reflectance with a maximum reflectance of  $60.3 \pm 3\%$  at 400 rpm (out of 5 repeated experimentations at the same condition)

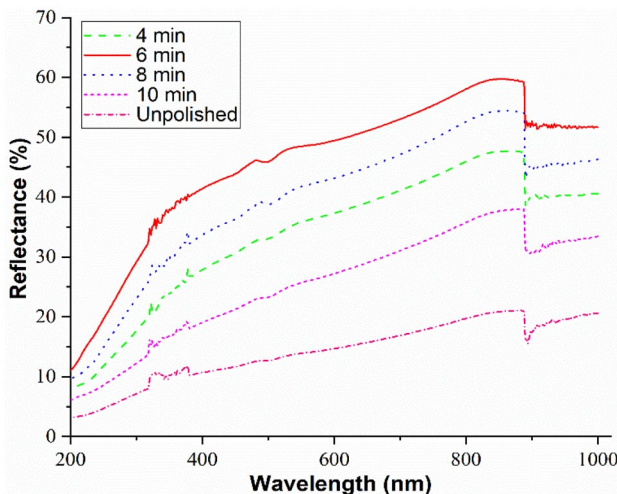


**Fig. 12** Effect of polishing time on surface reflectance with a maximum reflectance of  $59.7 \pm 3\%$  at 6 min (out of 5 repeated experimentations at the same condition)



**Fig. 13** Measured contact angles **a** before and **b** after EP

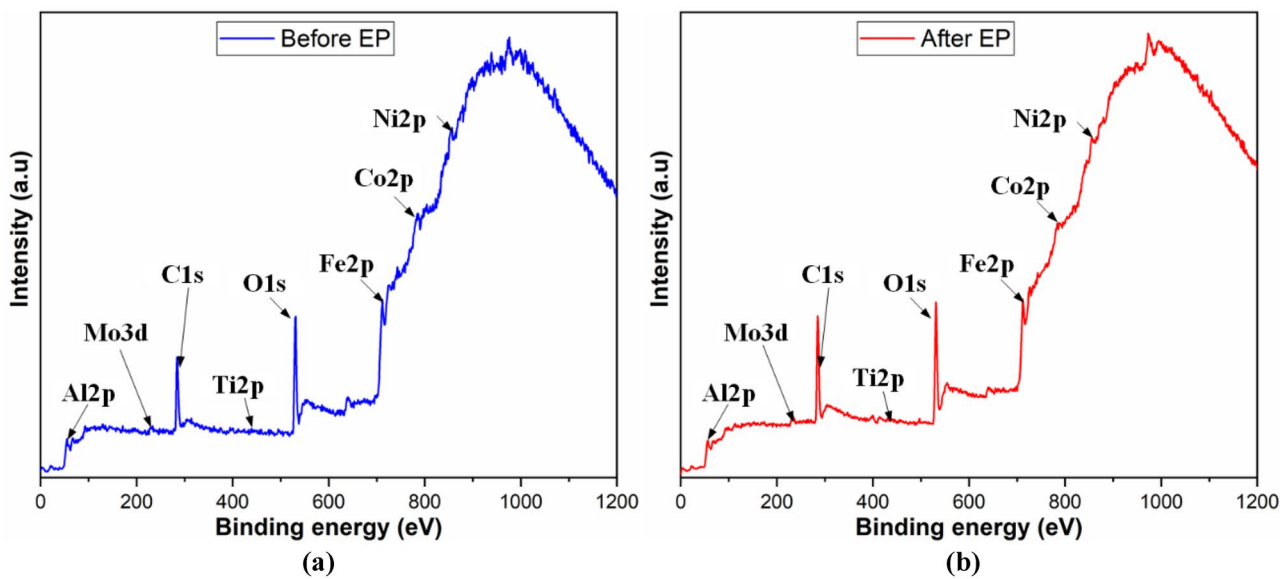
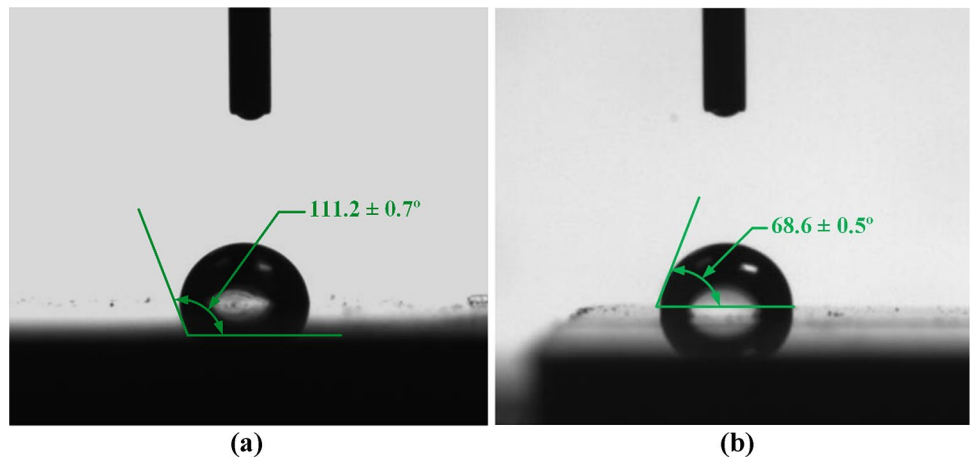


**Fig. 14** XPS spectra of maraging steel **a** before and **b** after EP

**Table 4** Elemental compositions of maraging steel from XPS spectra

Elements	Before EP		After EP	
	Binding energy (eV)	Atomic %	Binding energy (eV)	Atomic %
Fe2p	711.03	3.21	710.19	5.09
Al2p	70.28	0.37	74.09	0.7
Co2p	782.02	1.2	782.87	1.62
Mo3d	232.86	0.49	228.6	0.52
Ni2p	854.42	1.33	852.75	2.73
O1s	531.23	29.3	530.65	37.66
Ti2p	456.06	0.42	459.29	0.55
C1s	284.28	63.67	284.62	51.12

### 3.6 Effect of EP on workpiece surface wettability

From the present study, the best EP parameters are 60 °C temperature, 400 rpm of magnetic stirrer rotation, and 6 min of polishing time, at which experimentation is performed for contact angle analysis. The contact angle is measured by dropping a 2 μL water droplet on the workpiece surface before and after EP, as shown in Fig. 13. Five repeated sets of experimentations are performed. An angle of  $111.2 \pm 0.7^\circ$  ( $> 90^\circ$ ) is formed on the surface before EP (Fig. 13a), which signifies that the surface is hydrophobic. An angle of  $68.6 \pm 0.5^\circ$  ( $< 90^\circ$ ) is formed after EP (Fig. 13b), which indicates that the surface is hydrophilic. Electropolishing reduces surface

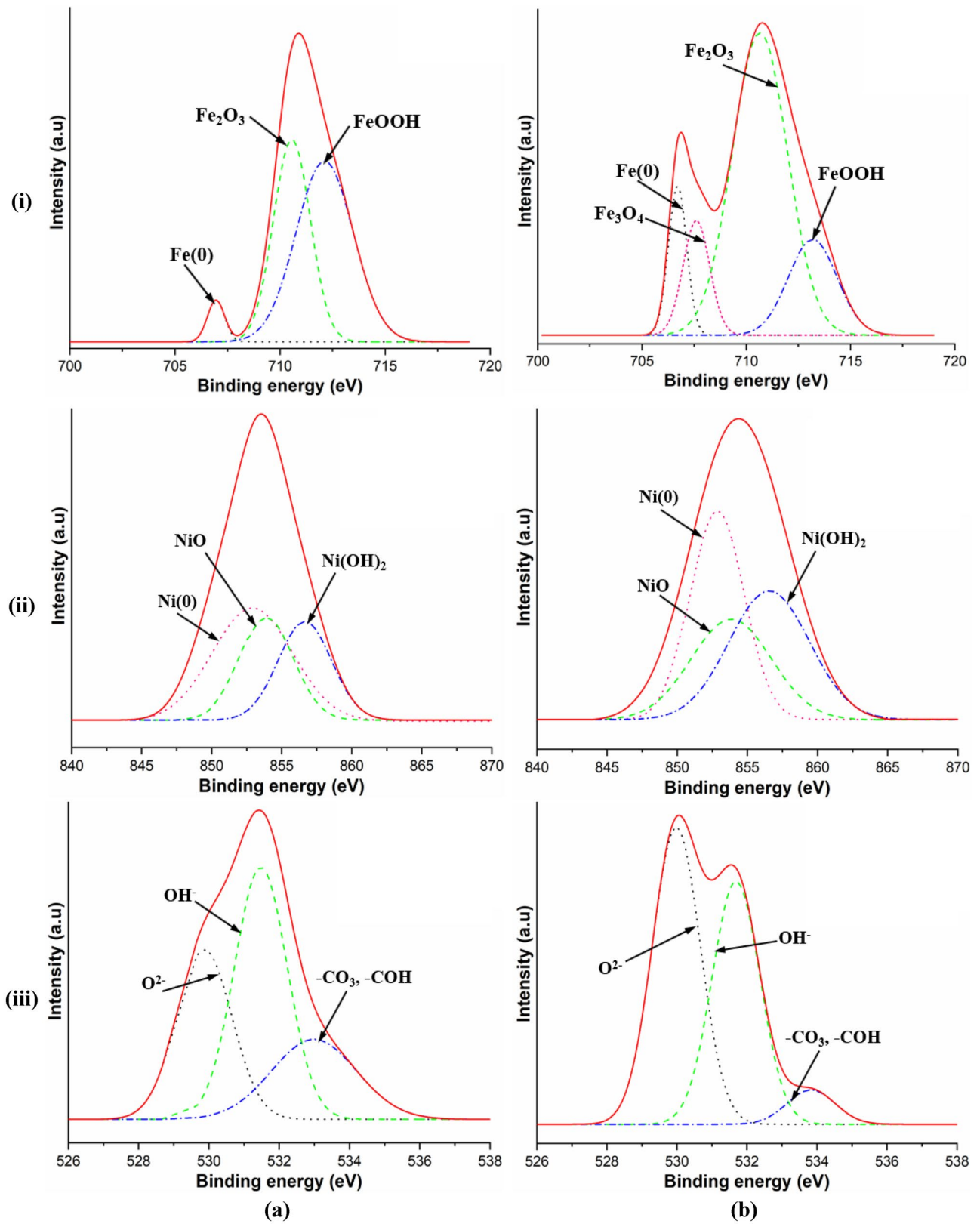


Fig. 15 High-resolution spectra of **i** iron, **ii** nickel, and **iii** oxygen elements **a** before and **b** after EP

irregularities and increases the wettability of the surface. Thus, EP changes the surface contact angle and makes it hydrophilic, which can be used in antifogging applications, biomedical, filtration, heat pipes, etc. [30].

### 3.7 XPS analysis of maraging steel

The surface elemental compositions of maraging steel before and after EP is studied with the help of XPS analysis, and the same is shown in Fig. 14. The surface scan is performed between 0 and 1200 eV with a step size of 1 eV. The surface consists of all the elements before and after EP. The peaks are matched with the results available in the literature [32].

Table 4 shows the elemental compositions of maraging steel obtained from the XPS spectra. It is noted that the oxygen O 1 s is the dominant element on both surfaces (both before and after EP) due to the passive oxide film present on the surface. From XPS analysis, it has been found that the percentage of the O 1 s element on the maraging steel surface is increased to 37.66% after electropolishing from its initial value of 29.3% (before electropolishing), which signifies that a thicker passive layer is formed after electropolishing. A similar observation was also found in the literature [26].

The major elements that participate in the passive layer formation are iron and nickel. The high-resolution spectra of (i) iron, (ii) nickel, and (iii) oxygen (a) before and (b) after EP are presented in Fig. 15 to analyze the surface composition. The high-resolution spectra of iron consist of three and four peaks before and after EP, respectively, as shown in Fig. 15i a, b. However, the peak of Fe(O) and Fe<sub>2</sub>O<sub>3</sub> has been increased after EP with a new peak of Fe<sub>3</sub>O<sub>4</sub>. Similar results were obtained by Han and Fang [26].

The high-resolution spectra of nickel before and after EP are shown in Fig. 15ii a, b, respectively, with the major compositions of Ni(0), NiO, and Ni(OH)<sub>2</sub>. After EP, all the major compositions are increased, which signifies a thicker passive layer. The high-resolution spectra of oxygen before and after EP are shown in Fig. 15iii a, b, respectively with the major compositions of O<sup>2-</sup> and OH<sup>-</sup>. However, after EP, the composition of O<sup>2-</sup> and OH<sup>-</sup> increases, leading to the generation of metal oxides/hydroxides [33]. The newly formed oxide layer increases the corrosion resistance after EP.

### 3.8 Effect of EP on corrosion behavior

The corrosion resistance of the maraging steel is an essential parameter for practical application. Potentiodynamic polarization curves measure the corrosion resistance of maraging steel before and after EP with 3.5 wt.% NaCl

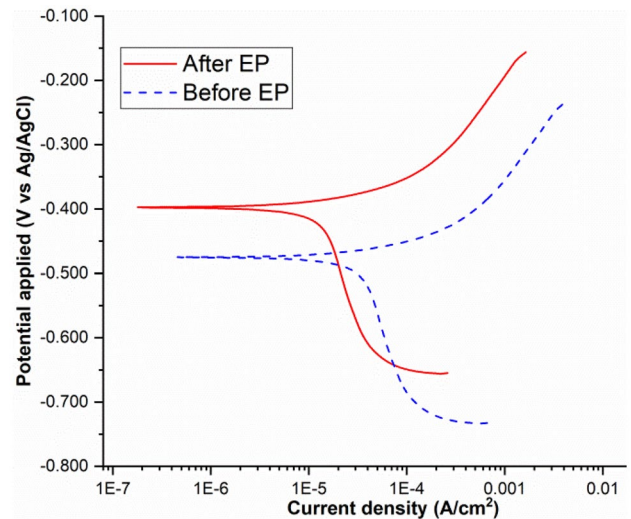


Fig. 16 Tafel polarization curve before and after EP

solution [20]. As shown in Fig. 16, a higher value of corrosion potential of maraging steel is observed after EP. However, the corrosion current density of maraging steel decreases from 16.5 to 6.84  $\mu\text{A}/\text{cm}^2$  after EP (Table 5), indicating higher corrosion resistance of electropolished maraging steel. Higher  $E_{\text{corr}}$  and lower  $I_{\text{corr}}$  values increase corrosion resistance [26, 34].

Surface reflectivity (Fig. 17i) and corresponding 3D surface profiles (Fig. 17ii) are shown (a) before and (b) after EP. EP is performed at 6 V, 60 °C, and 400 rpm for 6 min. It can be inferred from Fig. 17i that the surface reflectance and corresponding 3D surface profiles (Fig. 17ii) for the workpiece surface improved significantly (b) after EP compared to its (a) initial surface. The surface morphologies of the components are observed through FESEM images, as shown in Fig. 17iii (a) before and (b) after EP. It can be inferred that all the surface defects, like scratches, undulation, etc., got removed after EP (Fig. 17iii b).

To analyze the 2D surface roughness ( $R_a$ ) profiles before and after EP, both the profiles are plotted in the same graph as shown in Fig. 17iv. Electropolishing has reduced surface irregularities, and the corresponding surface roughness ( $R_a$ ) value is reduced to 0.119  $\mu\text{m}$  after EP from its initial value of 0.272  $\mu\text{m}$ .

Table 5 Potentiodynamic corrosion test result

Conditions	$E_{\text{corr}}$ (V vs. Ag/AgCl)	$I_{\text{corr}}$ ( $\mu\text{A}/\text{cm}^2$ )
Before EP	-0.475	16.5
After EP	-0.397	6.84

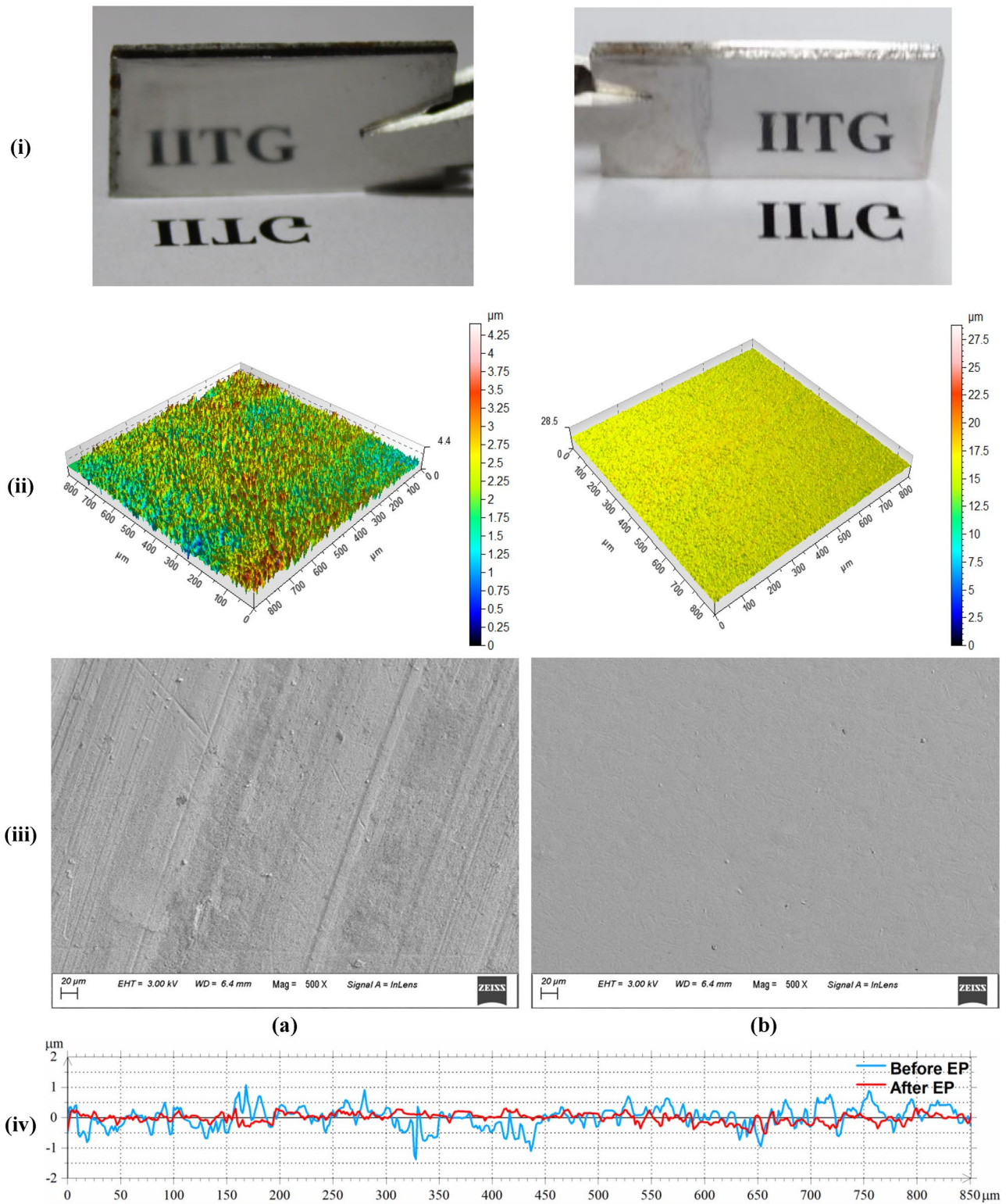


**Fig. 17** i Surface reflectance, ii 3D surface roughness profiles, and iii surface morphology a before and b after EP; iv 2D surface roughness profiles



## 4 Conclusions

Electropolishing of maraging steel is performed with acetic acid and perchloric acid mixed in a volume ratio of 3:1. Effects of various input parameters of EP are investigated, and results are compared before and after EP.

- The EDS analysis shows that the nickel and oxygen concentrations on EP polished surface increase.
- Electropolishing at 60 °C, with the magnetic stirrer rotation at 400 rpm and polishing time of 6 min, gives a maximum improvement of 56.25% in surface roughness and 60.3% in surface reflectance.
- The contact angle is changed from 111.2 to 68.6° after EP. It is observed that EP makes the surface hydrophilic.
- XPS analysis suggests that the passive layer is formed after EP, improving corrosion resistance.
- EP improves the corrosion resistance as  $E_{\text{corr}}$  shifts from  $-0.475$  to  $-0.397$  V, and  $I_{\text{corr}}$  shifts from 16.5 to 6.84  $\mu\text{A}/\text{cm}^2$  after EP. A more positive  $E_{\text{corr}}$  and lesser  $I_{\text{corr}}$  signifies increased corrosion resistance.

**Acknowledgements** The authors acknowledge the Department of Physics, Indian Institute of Technology Guwahati, India, for providing the UV spectrometer for the surface reflectance analysis.

**Author contribution** Abhinav Kumar - conceptualization, methodology, visualization, and writing the original draft; Suraj Kumar - data collection and experimental investigation; Manas Das—conceptualization, resources, reviewing, and editing.

**Availability of data and material** There is no other associated data.

**Code availability** Not applicable.

## Declarations

**Ethics approval** Not applicable.

**Consent to participate** Not applicable.

**Consent for publication** Not applicable.

**Competing interests** The authors declare no competing interests.

## References

- Jacquet PA (1936) The mechanism of electrolytic polishing of Copper. *CR Acad Sci* 202:402
- Lee SJ, Lai JJ (2003) The effects of electropolishing (EP) process parameters on corrosion resistance of 316L stainless steel. *J Mater Process Technol* 140(1–3):206–210
- Srinivasan PB, Marikkannu C, Ramu S, Balakrishnan K (1994) Corrosion of maraging steels in chloride solutions. *Br Corros J* 29(2):132–135
- Lee ES (2000) Machining characteristics of the electropolishing of stainless steel (STS316L). *Int J Adv Manuf Technol* 16(8):591–599
- Han W, Fang F (2019) Fundamental aspects and recent developments in electropolishing. *Int J Mach Tools Manuf* 139(April):1–23
- Poornima T, Nayak J, Shetty AN (2011) Effect of 4-(N,N-diethylamino) benzaldehyde thiosemicarbazone on the corrosion of aged 18 Ni 250 grade maraging steel in phosphoric acid solution. *Corros Sci* 53(11):3688–3696
- Ansell TY, Ricks JP, Park C, Tipper CS, Luhrs CC (2020) Mechanical properties of 3D-printed maraging steel induced by environmental exposure. *Metals (Basel)* 10(2):218
- Oliveira AR, Jardini AL, Del Conte EG (2020) Effects of cutting parameters on roughness and residual stress of maraging steel specimens produced by additive manufacturing. *Int J Adv Manuf Technol* 111(9–10):2449–2459
- Li B, Ding Z, Xiao J, Liang SY (2015) Maraging steel 3J33 phase transformation during micro-grinding. *Mater Lett* 164:217–220
- Huang CA, Chen YC, Chang JH (2008) The electrochemical polishing behavior of the Inconel 718 alloy in perchloric-acetic mixed acids. *Corros Sci* 50(2):480–489
- Huang CA, Chen YC (2009) The effect of water content on the electropolishing behavior of Inconel 718 alloy in perchloric-acetic acid mixtures. *Corros Sci* 51(9):1901–1906
- Aksu Y, Erdoğan M, Demirci G, Karakaya İ (2016) Electropolishing of an Fe-Ni-Co alloy in acetic acid-perchloric acid mixture. *ECS Trans* 72(22):13
- Wang G, Liu Z, Niu J, Huang W, Wang B (2020) Effect of electrochemical polishing on surface quality of nickel-titanium shape memory alloy after milling. *J Mater Res Technol* 9(1):253–262
- Han W, Fang F (2020) Eco-friendly NaCl-based electrolyte for electropolishing 316L stainless steel. *J Manuf Process* 58(October):1257–1269
- Wang K, Yan Y, Zhou P, Zhang C, Kang R, Guo D (2020) Preparation of flat and smooth copper surface by jet electrochemical machining and electrochemical polishing. *J Electrochem Soc* 167(16):163501
- Piotrowski O, Madore C, Landolt D (1998) The mechanism of electropolishing of titanium in methanol-sulfuric acid electrolytes. *J Electrochem Soc* 145(7):2362
- Zhao T, Wang S, Liu Z, Du C, Li X (2021) Effect of cathodic polarisation on stress corrosion cracking behaviour of a Ni(Fe, Al)-maraging steel in artificial seawater. *Corros Sci* 179:109176
- Barman A, Das M (2018) Nano-finishing of bio-titanium alloy to generate different surface morphologies by changing magnetorheological polishing fluid compositions. *Precis Eng* 51:145–152
- Rudawska A, Jacniacka E (2018) Evaluating uncertainty of surface free energy measurement by the van Oss-Chaudhury-Good method. *Int J Adhes Adhes* 82:139–145
- Hou Y, Li R, Liang J, Su P, Ju P (2018) Electropolishing of Al and Al alloys in AlCl<sub>3</sub>/trimethylamine hydrochloride ionic liquid. *Surf Coatings Technol* 335:72–79
- Urlea V, Brailovski V (2017) Electropolishing and electropolishing-related allowances for IN625 alloy components fabricated by laser powder-bed fusion. *Int J Adv Manuf Technol* 92(9–12):4487–4499
- Taylor PB, Agrawal A, Joshi SS (2015) Numerical modeling of passive layer formation and stabilization in electrochemical polishing process. *J Manuf Process* 18:107–116
- Latifi A, Imani M, Khorasani MT, Joupri MD (2013) Electrochemical and chemical methods for improving surface characteristics of 316L stainless steel for biomedical applications. *Surf Coatings Technol* 221:1–12
- Tran T, Brown B, Nestic S, Tribollet B (2013) Investigation of the mechanism for acetic acid corrosion of mild steel. *Corrosion* 70(3):1–12

25. Tyagi P, Goulet T, Brent D, Klein K, Garcia-Moreno F (2018) Scanning electron microscopy and optical profilometry of electropolished additively manufactured 316 steel components. ASME International Mechanical Engineering Congress and Exposition 52019:V002T02A019
26. Han W, Fang F (2019) Electropolishing of 316L stainless steel using sulfuric acid-free electrolyte. *J Manuf Sci Eng* 141(10)
27. Haidopoulos M, Turgeon S, Sarra-Bournet C, Laroche G, Mantovani D (2006) Development of an optimized electrochemical process for subsequent coating of 316 stainless steel for stent applications. *J Mater Sci Mater Med* 17(7):647–657
28. Félix-Martínez C, Ibarra-Medina J, Fernández-Benavides DA, Cáceres-Díaz LA, Alvarado-Orozco JM (2021) Effect of the parametric optimization and heat-treatment on the 18Ni-300 maraging steel microstructural properties manufactured by directed energy deposition. *Int J Adv Manuf Technol* 115(11–12):3999–4020
29. Kumar A, Das M (2021) Multiphysics simulation and experimental investigation of microtool fabricated by EMM. *Mater Manuf Process* 36(13):1489–1500
30. Tyagi P et al (2020) Roughness reduction of additively manufactured steel by electropolishing. *Int J Adv Manuf Technol* 106(3–4):1337–1344
31. Habibzadeh S, Li L, Shum-Tim D, Davis EC, Omanovic S (2014) Electrochemical polishing as a 316L stainless steel surface treatment method: towards the improvement of biocompatibility. *Corros Sci* 87:89–100
32. Yan J, Zhou Y, Gu R, Zhang X, Quach WM, Yan M (2019) A comprehensive study of steel powders (316L, H13, P20 and 18Ni300) for their selective laser melting additive manufacturing
33. Han W, Fang F (2020) Two-step electropolishing of 316L stainless steel in a sulfuric acid-free electrolyte. *J Mater Process Technol* 279:116558
34. Pal A, Das C (2020) A novel use of solid waste extract from tea factory as corrosion inhibitor in acidic media on boiler quality steel. *Ind Crops Prod* 151:112468

**Publisher's Note** Springer Nature remains neutral with regard to jurisdictional claims in published maps and institutional affiliations.